

Exclusive ρ^0 electroproduction on transversely polarized protons

A. Airapetian,^{12,15} N. Akopov,²⁶ Z. Akopov,²⁶ E.C. Aschenauer,⁶ W. Augustyniak,²⁵ A. Avetissian,²⁶ E. Avetisyan,⁵ B. Ball,¹⁵ N. Bianchi,¹⁰ H.P. Blok,^{17,24} H. Böttcher,⁶ C. Bonomo,⁹ A. Borissoy,⁵ V. Bryzgalov,¹⁹ J. Burns,¹³ M. Capiluppi,⁹ G.P. Capitani,¹⁰ E. Cisbani,²¹ G. Ciullo,⁹ M. Contalbrigo,⁹ P.F. Dalpiaz,⁹ W. Deconinck,^{5,15} R. De Leo,² L. De Nardo,^{5,15} E. De Sanctis,¹⁰ M. Diefenthaler,^{14,8} P. Di Nezza,¹⁰ J. Dreschler,¹⁷ M. Düren,¹² M. Ehrenfried,¹² G. Elbakian,²⁶ F. Ellinghaus,⁴ R. Fabbri,⁶ A. Fantoni,¹⁰ L. Fellowka,²² S. Frullani,²¹ D. Gabbert,⁶ G. Gapienko,¹⁹ V. Gapienko,¹⁹ V. Gharibyan,²⁶ F. Giordano,^{5,9} S. Gliske,¹⁵ C. Hadjidakis,¹⁰ M. Hartig,⁵ D. Hasch,¹⁰ G. Hill,¹³ A. Hillenbrand,⁶ M. Hoek,¹³ Y. Holler,⁵ I. Hristova,⁶ Y. Imazu,²³ A. Ivanilov,¹⁹ H.E. Jackson,¹ H.S. Jo,¹¹ S. Joosten,^{14,11} R. Kaiser,¹³ T. Keri,^{13,12} E. Kinney,⁴ A. Kisselev,¹⁸ N. Kobayashi,²³ V. Korotkov,¹⁹ P. Kravchenko,¹⁸ L. Lagamba,² R. Lamb,¹⁴ L. Lapikás,¹⁷ I. Lehmann,¹³ P. Lenisa,⁹ L.A. Linden-Levy,¹⁴ A. López Ruiz,¹¹ W. Lorenzon,¹⁵ X.-G. Lu,⁶ X.-R. Lu,²³ B.-Q. Ma,³ D. Mahon,¹³ N.C.R. Makins,¹⁴ S.I. Manaenkov,¹⁸ L. Manfré,²¹ Y. Mao,³ B. Marianski,²⁵ A. Martinez de la Ossa,⁴ H. Marukyan,²⁶ C.A. Miller,²² Y. Miyachi,²³ A. Movsisyan,²⁶ V. Muccifora,¹⁰ M. Murray,¹³ A. Mussgiller,^{5,8} E. Nappi,² Y. Naryshkin,¹⁸ A. Nass,⁸ W.-D. Nowak,⁶ L.L. Pappalardo,⁹ R. Perez-Benito,¹² P.E. Reimer,¹ A.R. Reolon,¹⁰ C. Riedl,⁶ K. Rith,⁸ G. Rosner,¹³ A. Rostomyan,⁵ J. Rubin,¹⁴ D. Ryckbosch,¹¹ Y. Salomatin,¹⁹ F. Sanftl,²⁰ A. Schäfer,²⁰ G. Schnell,^{6,11} K.P. Schüller,⁵ B. Seitz,¹³ T.-A. Shibata,²³ V. Shutov,⁷ M. Stancari,⁹ M. Statera,⁹ E. Steffens,⁸ J.J.M. Steijger,¹⁷ H. Stenzel,¹² J. Stewart,⁶ F. Stinzinger,⁸ S. Taroian,²⁶ A. Terkulov,¹⁶ A. Trzcinski,²⁵ M. Tytgat,¹¹ A. Vandenbroucke,¹¹ P.B. van der Nat,¹⁷ Y. Van Haarlem,¹¹ C. Van Hulse,¹¹ M. Varanda,⁵ D. Veretennikov,¹⁸ V. Vikhrov,¹⁸ I. Vilardi,² C. Vogel,⁸ S. Wang,³ S. Yaschenko,^{6,8} H. Ye,³ Z. Ye,⁵ S. Yen,²² W. Yu,¹² D. Zeiler,⁸ B. Zihlmann,⁵ and P. Zupranski²⁵

(The HERMES Collaboration)

¹Physics Division, Argonne National Laboratory, Argonne, Illinois 60439-4843, USA

²Istituto Nazionale di Fisica Nucleare, Sezione di Bari, 70124 Bari, Italy

³School of Physics, Peking University, Beijing 100871, China

⁴Nuclear Physics Laboratory, University of Colorado, Boulder, Colorado 80309-0390, USA

⁵DESY, 22603 Hamburg, Germany

⁶DESY, 15738 Zeuthen, Germany

⁷Joint Institute for Nuclear Research, 141980 Dubna, Russia

⁸Physikalisches Institut, Universität Erlangen-Nürnberg, 91058 Erlangen, Germany

⁹Istituto Nazionale di Fisica Nucleare, Sezione di Ferrara and

Dipartimento di Fisica, Università di Ferrara, 44100 Ferrara, Italy

¹⁰Istituto Nazionale di Fisica Nucleare, Laboratori Nazionali di Frascati, 00044 Frascati, Italy

¹¹Department of Subatomic and Radiation Physics, University of Gent, 9000 Gent, Belgium

¹²Physikalisches Institut, Universität Gießen, 35392 Gießen, Germany

¹³Department of Physics and Astronomy, University of Glasgow, Glasgow G12 8QQ, United Kingdom

¹⁴Department of Physics, University of Illinois, Urbana, Illinois 61801-3080, USA

¹⁵Randall Laboratory of Physics, University of Michigan, Ann Arbor, Michigan 48109-1040, USA

¹⁶Lebedev Physical Institute, 117924 Moscow, Russia

¹⁷National Institute for Subatomic Physics (Nikhef), 1009 DB Amsterdam, The Netherlands

¹⁸Petersburg Nuclear Physics Institute, Gatchina, Leningrad region, 188300 Russia

¹⁹Institute for High Energy Physics, Protvino, Moscow region, 142281 Russia

²⁰Institut für Theoretische Physik, Universität Regensburg, 93040 Regensburg, Germany

²¹Istituto Nazionale di Fisica Nucleare, Sezione Roma 1, Gruppo Sanità and Physics Laboratory, Istituto Superiore di Sanità, 00161 Roma, Italy

²²TRIUMF, Vancouver, British Columbia V6T 2A3, Canada

²³Department of Physics, Tokyo Institute of Technology, Tokyo 152, Japan

²⁴Department of Physics and Astronomy, Vrije Universiteit, 1081 HV Amsterdam, The Netherlands

²⁵Andrzej Soltan Institute for Nuclear Studies, 00-689 Warsaw, Poland

²⁶Yerevan Physics Institute, 375036 Yerevan, Armenia

(Dated: October 23, 2018)

The exclusive electroproduction of ρ^0 mesons was studied with the HERMES spectrometer at the DESY laboratory by scattering 27.6 GeV positron and electron beams off a transversely polarized hydrogen target. Spin density matrix elements for this process were determined from the measured production- and decay-angle distributions of the produced ρ^0 mesons. These matrix elements embody information on helicity transfer and the validity of s -channel helicity conservation in the case of a transversely polarized target. From the spin density matrix elements, the leading-twist term

in the single-spin asymmetry was calculated separately for longitudinally and transversely polarized ρ^0 mesons. Neglecting s -channel helicity changing matrix elements, results for the former can be compared to calculations based on generalized parton distributions, which are sensitive to the contribution of the total angular momentum of the quarks to the proton spin.

PACS numbers: 13.60.Le, 13.88.+e, 14.20.Dh, 14.40.Aq, 12.38.Qk

Exclusive electroproduction of mesons can provide new information about the structure of the nucleon because of its relation to generalized parton distributions (GPDs) [1, 2, 3]. In Ref. [4] it has been proven that the amplitude for hard exclusive electroproduction of mesons by longitudinal virtual photons can be factorized into a hard-scattering part and a soft part that depends on the structure of the nucleon and the produced meson. In the case of exclusive vector meson production, also the produced meson is longitudinally polarized (in addition to the virtual photon being longitudinal). The amplitude for the soft part can be expressed in terms of GPDs.

GPDs provide a three-dimensional representation of the structure of the nucleon at the partonic level, correlating the longitudinal momentum fraction of a parton with its transverse spatial coordinates. They are related to the standard parton distribution functions and nucleon form factors [3, 5, 6, 7]. At leading twist, meson production is described by four types of GPDs: $H^{q,g}$, $E^{q,g}$, $\tilde{H}^{q,g}$, and $\tilde{E}^{q,g}$, where q stands for a quark flavour and g for a gluon. The GPDs are functions of t , x , and ξ , where t is the squared four-momentum transfer to the nucleon, x the average, and ξ half the difference of the longitudinal momentum fractions of the quark or gluon in the initial and final state. The quantum numbers of the produced meson determine the sensitivity to the various GPDs. In particular, at leading twist, production of vector mesons is sensitive only to the GPDs H^q , E^q , H^g , and E^g .

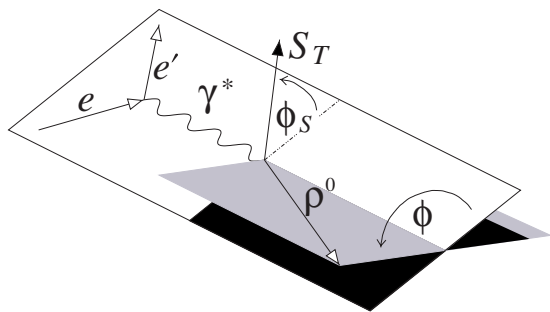


FIG. 1: The lepton scattering and hadron production planes together with the azimuthal angles ϕ and ϕ_S .

The transverse target-spin asymmetry in exclusive electroproduction of longitudinally polarized vector mesons by longitudinal virtual photons is an important observable, because it depends almost linearly on the GPD E [5]. This is in contrast to the unpolarized cross

section, where the contribution of E is generally small compared to the contribution of H . At leading twist, the asymmetry is proportional to $\sin(\phi - \phi_S)$, where ϕ and ϕ_S are the azimuthal angles about the virtual-photon direction of the hadron production plane and the transverse part \vec{S}_T of the target spin, respectively, with respect to the lepton scattering plane (see Fig. 1).

The cross section and asymmetry for exclusive ρ^0 electroproduction $e + p \rightarrow e' + \rho^0 + p'$ can conveniently be described using spin density matrix elements [9, 10, 11]. By using the angular distribution of the produced vector meson and of its decay products, as described by the polar and azimuthal angles ϑ and φ (see Fig. 2), one can separate the contributions of mesons with longitudinal and transverse polarization to the measured asymmetries. If s -channel helicity conservation (SCHC) holds, the helicity of the virtual photon is transferred to the produced vector meson. In that case studying the asymmetry for the production of longitudinally polarized vector mesons is tantamount to selecting longitudinal virtual photons. Measurements have shown that SCHC holds reasonably well for exclusive electroproduction of ρ^0 mesons on an unpolarized target at HERMES kinematics [12]. Thus information on the GPD E can be obtained from measurements of the transverse target-spin asymmetry in exclusive ρ^0 electroproduction.

Ultimately, these studies will help to understand the origin of the nucleon spin, because it has been shown [3] that the x -moment in the limit $t \rightarrow 0$ of the sum of the GPDs H^q and E^q is related to the contribution J^q of the total angular momentum of the quark with flavour q to the nucleon spin.

In this paper, measurements of exclusive ρ^0 electroproduction on transversely polarized protons are presented. For the first time, values of the spin density matrix elements (SDMEs) and the transverse target-spin asymmetry for this process were determined.

The data were collected with the HERMES spectrometer [13] during the period 2002 – 2005. The 27.6 GeV HERA electron or positron beam at DESY scattered off a transversely polarized hydrogen target [14] of which the spin direction was reversed every 1 – 3 minutes. The average magnitude of the target polarization was $|P_T| = 0.724 \pm 0.059$. The lepton beam was longitudinally polarized, the helicity being reversed periodically. The net polarization for the selected data was 0.095 ± 0.005 , mainly because more data were taken with positive helicity.

Leptons were distinguished from hadrons with an av-

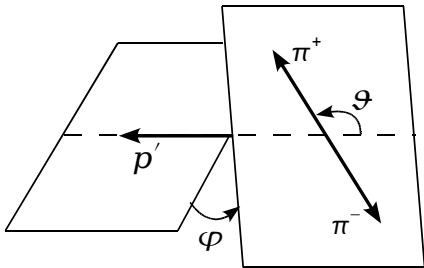


FIG. 2: The polar and azimuthal angles of the decay π^+ of the ρ^0 in the ρ^0 rest frame. The positive z -axis is taken opposite to the direction of the residual proton, while the angle φ is defined with respect to the hadron production plane.

erage efficiency of 98% and a hadron contamination of less than 1% by using the information from an electromagnetic calorimeter, a transition-radiation detector, a preshower scintillation counter, and a Ring Imaging Čerenkov detector. Events were selected in which only one lepton and two oppositely charged hadrons were detected.

In the event selection, the following kinematic constraints were imposed: $Q^2 > 1 \text{ GeV}^2$, $W^2 > 4 \text{ GeV}^2$, and $-t' < 0.4 \text{ GeV}^2$. Here $-Q^2$ is the squared four-momentum of the exchanged virtual photon, W the invariant mass of the virtual-photon proton system, and t' the reduced Mandelstam variable $t' = t - t_0$, where $-t_0$ is the minimum value of $-t$ for a given value of Q^2 and the Bjorken variable x_B . The average value of W^2 for the exclusive ρ^0 sample was 25 GeV^2 . The condition on t' was applied to reduce non-exclusive background.

An exclusive event sample was selected by constraining the value of the variable

$$\Delta E = \frac{M_X^2 - M^2}{2M}, \quad (1)$$

where M_X is the missing mass and M the proton mass. The measured ΔE distribution, which includes constraints on the invariant mass of the produced hadron pair as discussed below, is shown in Fig. 3. The peak around zero originates from the exclusive reaction. Exclusive events were selected by the requirement $\Delta E < 0.6 \text{ GeV}$. This resulted in a total number of 7488 events. The background from non-exclusive processes in the exclusive region was estimated by using a PYTHIA6 Monte Carlo simulation [15, 16] in conjunction with a special set of JETSET fragmentation parameters, tuned to provide an accurate description of deep-inelastic hadron production in the HERMES kinematic domain [17, 18]. The simulation gave a very good description of the ΔE distribution in the non-exclusive region. The background fractions in the exclusive region varied between 7% and 23%, depending on the value of Q^2 , x_B , or t' , with an average over all selected data of 11%.

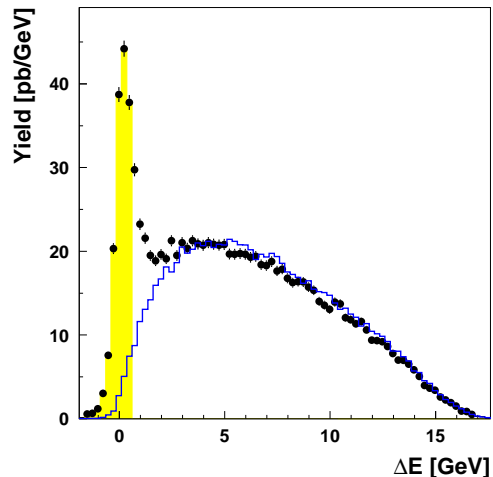


FIG. 3: The ΔE distributions of the measured yield (number of counts within the acceptance divided by the integrated luminosity) (dots) and a Monte Carlo simulation with PYTHIA6 of the non-exclusive background normalized to the same integrated luminosity (histogram). The kinematic cuts and the requirements $0.6 \text{ GeV} < M_{\pi\pi} < 1.0 \text{ GeV}$ and $M_{KK} > 1.04 \text{ GeV}$ were applied. The selected exclusive region is indicated by the dashed area.

The invariant mass of the two-hadron system $M_{\pi\pi}$ was determined assuming that both hadrons are pions. Resonant $\pi^+\pi^-$ pairs, i.e., pairs produced in the decay $\rho^0 \rightarrow \pi^+\pi^-$, were selected by the condition $0.6 \text{ GeV} < M_{\pi\pi} < 1.0 \text{ GeV}$. Contributions in the $M_{\pi\pi}$ spectrum from the decay of a ϕ meson into two kaons were excluded by requiring $M_{KK} > 1.04 \text{ GeV}$, where M_{KK} is the invariant mass of the two-hadron system calculated assuming that both hadrons are kaons. After subtracting the simulated contribution from the non-exclusive tail in the region $\Delta E < 0.6 \text{ GeV}$ and correcting for the non-constant acceptance with $M_{\pi\pi}$, the $M_{\pi\pi}$ spectrum for exclusive events was fitted with a ρ^0 -peak plus a linear background. For the shape of the ρ^0 -peak Söding and Ross-Stodolsky parametrizations were used. In both cases the resulting background was found to be negligible ($0.7 \pm 0.5\%$).

In the analysis the recently developed formalism for electroproduction of a vector meson from a polarized nucleon was used [11]. The cross section for exclusive ρ^0 leptonproduction is written as

$$\frac{1}{(2\pi)^2} \frac{d\sigma}{dx_B dQ^2 dt} W(x_B, Q^2, t, \phi, \phi_S, \varphi, \vartheta) = \frac{d\sigma}{d\psi d\phi d\varphi d(\cos\vartheta) dx_B dQ^2 dt} = \quad (2)$$

with ψ being a similar angle as ϕ_S , but now defined around the direction of the lepton beam, and

$$\frac{d\sigma}{dx_B dQ^2 dt} = \Gamma_v \left(\frac{d\sigma_T}{dt} + \varepsilon \frac{d\sigma_L}{dt} \right), \quad (3)$$

where Γ_v is the virtual photon flux factor in the Hand convention [19], ε is the virtual-photon polarization parameter, and $d\sigma_T/dt$ and $d\sigma_L/dt$ are the usual x_B, Q^2 , and t dependent γ^*p cross sections for transverse and longitudinal virtual photons, respectively.

The function $W(x_B, Q^2, t, \phi, \phi_S, \varphi, \vartheta)$ describes the angular distribution of both the produced ρ^0 and its decay pions. It consists of several terms corresponding to different polarizations of the incoming lepton beam and the target nucleon:

$$W = W_{UU} + P_\ell W_{LU} + S_L W_{UL} + P_\ell S_L W_{LL} + S_T W_{UT} + P_\ell S_T W_{LT}, \quad (4)$$

where the left (right) subscript specifies the beam (target) polarization: unpolarized (U), longitudinally (L), or transversely (T) polarized, and P_ℓ , S_L , and S_T represent the longitudinal polarization of the beam, and the longitudinal and transverse polarization of the target (with respect to the virtual photon direction), respectively.

For the case of zero beam polarization and only transverse target polarization¹ the angular-distribution function reads

$$W(\phi, \phi_S, \varphi, \vartheta) = W_{UU}(\phi, \varphi, \vartheta) + S_T W_{UT}(\phi, \phi_S, \varphi, \vartheta). \quad (5)$$

Here and in the following the dependence of the various angular distribution functions W on x_B, Q^2 , and t is omitted for the sake of legibility.

The functions W_{UY} (with $Y = U, T$) can be further decomposed into terms corresponding to specific ρ^0 polarizations, indicated by the superscripts, according to

$$W_{UY}(\phi_S, \phi, \varphi, \vartheta) = \frac{3}{4\pi} \left[\cos^2 \vartheta W_{UY}^{LL}(\phi_S, \phi) + \sqrt{2} \cos \vartheta \sin \vartheta W_{UY}^{LT}(\phi_S, \phi, \varphi) + \sin^2 \vartheta W_{UY}^{TT}(\phi_S, \phi, \varphi) \right]. \quad (6)$$

Note that in the case of W_{UU} there is no dependence on ϕ_S . The production of a longitudinally polarized ρ^0 is described by W_{UY}^{LL} , the production of a transversely polarized ρ^0 (including the interference from amplitudes with positive and negative ρ^0 helicity) by W_{UY}^{TT} , while W_{UY}^{LT} results from the interference between longitudinal and transverse ρ^0 polarizations.

The terms W_{UY}^{AB} can be expanded (see Eqs. 4.10 and 4.17 of Ref. [11]) into trigonometric functions of the angles ϕ_S, ϕ , and φ , where the coefficients are SDMEs (or combinations thereof) $u_{\mu\mu'}^{\nu\nu'}$ for W_{UU}^{AB} , and $n_{\mu\mu'}^{\nu\nu'}$ and $s_{\mu\mu'}$

for W_{UT}^{AB} . Here the letters u, n , and s stand for unpolarized, normal, and sideways (with respect to the direction of the virtual photon and the electron scattering plane) target polarization, and the sub(super)scripts refer to the helicity of the virtual photon (ρ^0 meson) in the helicity amplitudes that occur in the SDMEs. In the case of W_{UU} there are 15 independent terms in the expansion. There is a direct relation between these SDMEs and the ones in the Schilling-Wolf formalism [9]. For W_{UT} the expansion contains 30 independent terms.

First the 15 ‘unpolarized’ SDMEs of W_{UU} were determined by fitting the angular distributions of the combined events for the two target polarization states. The fit was performed by maximum-likelihood estimation with a probability density function

$$f_U(\phi, \varphi, \vartheta) = \mathcal{N}_U^{-1} \mathcal{A}(\phi, \varphi, \vartheta) W_{UU}(\phi, \varphi, \vartheta), \quad (7)$$

where the function \mathcal{A} represents the acceptance of the HERMES spectrometer. The factor \mathcal{N}_U represents the normalization integral of the probability density function, which was computed numerically using Monte Carlo events that are within the acceptance of the spectrometer. The non-exclusive background was included in the fit function using fixed effective values of the SDMEs for this background. The latter were obtained from a fit of the angular distribution of the PYTHIA6 Monte Carlo events for $\Delta E < 0.6$ GeV. The results for the 15 unpolarized SDMEs, which as mentioned are for data taken in the years 2002–2005, are fully consistent with those from the analysis of all data taken in the period 1996–2005 using the Schilling-Wolf formalism [12].

Then the 30 SDMEs W_{UT} were determined, keeping the unpolarized SDMEs fixed to the values found in the fit of W_{UU} described above, using the probability density function

$$f_T(\phi, \phi_S, \varphi, \vartheta) = \mathcal{N}_T^{-1} \mathcal{A}(\phi, \phi_S, \varphi, \vartheta) \times (W_{UU}(\phi, \varphi, \vartheta) + P_T W_{UT}(\phi, \phi_S, \varphi, \vartheta)). \quad (8)$$

A factor $d\psi/d\phi_S$, which takes into account that the yields are evaluated differentially in the angle ϕ_S , rather than in ψ , was left out, since it was very close to unity. As in the unpolarized case, the background was included in the fit. Since nothing is known about the asymmetry of the background, the 30 SDMEs for the background were taken to be zero, and the possible influence of this assumption was included in the systematic uncertainties.

Besides the target polarization, various other sources of systematic uncertainties for the SDMEs and asymmetries extracted were investigated and evaluated. In most cases the resulting systematic uncertainties were found to be negligible, i.e., very small compared to the statistical uncertainty. These include the effect of radiative corrections and the uncertainties resulting from the uncertainty in the unpolarized SDMEs and the background

¹ Because the target polarization is transverse to the incoming beam, there is a small longitudinal polarization with respect to the direction of the virtual photon. The effect of the latter and of a small longitudinal polarization of the beam will be discussed later.

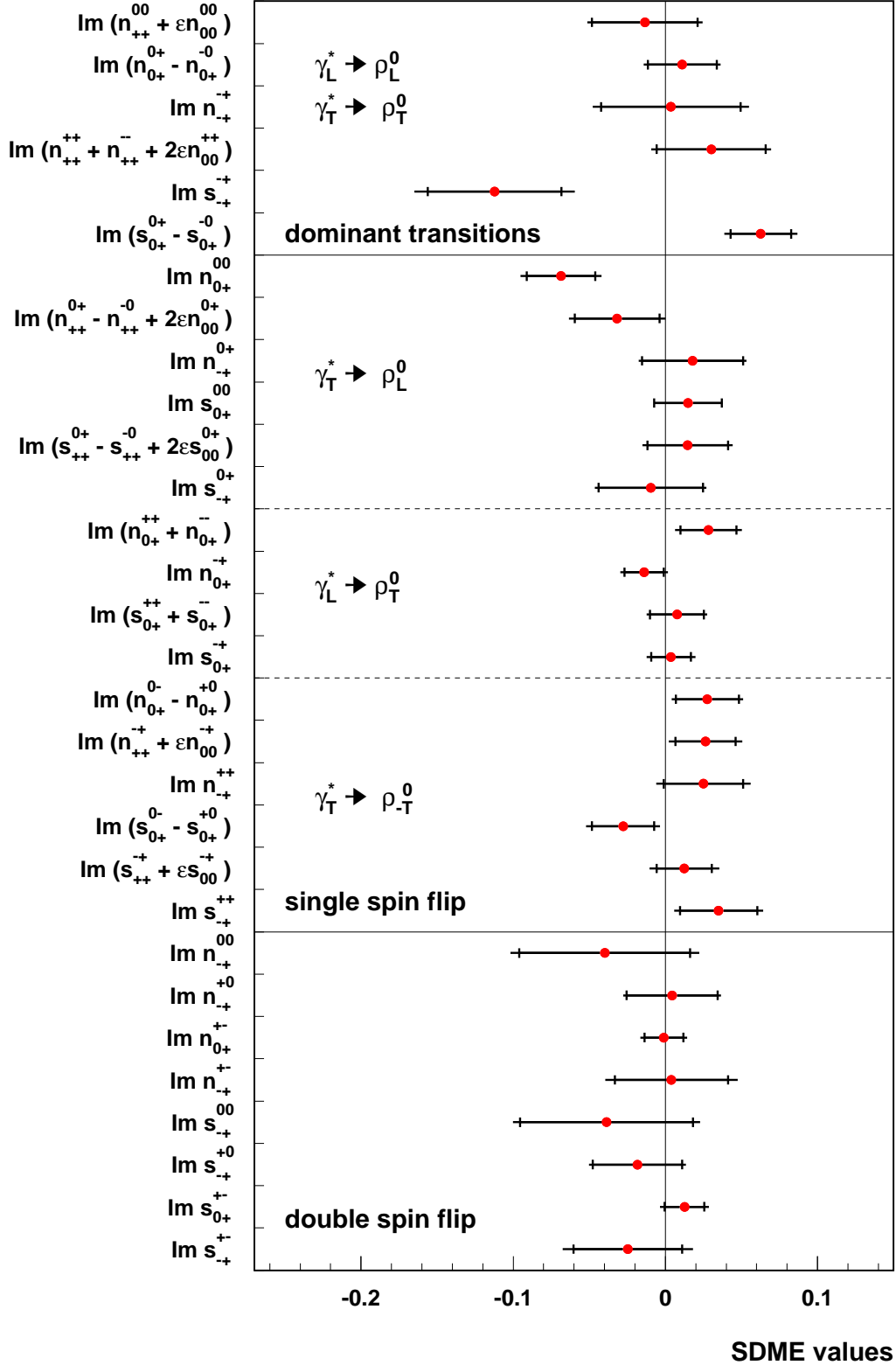


FIG. 4: Values of SDMEs, or combinations thereof, for a transversely polarized proton target and an unpolarized beam. The SDMEs are sorted into three categories, which are separated from each other by the solid horizontal lines. From top to bottom: SDMEs containing s -channel helicity-conserving amplitudes, combinations containing at least one s -channel helicity-changing amplitude, and SDMEs containing two s -channel helicity-changing amplitudes. Within the second category the combinations are sorted into three groups associated with different virtual photon and ρ^0 polarizations. The inner error bars represent the statistical uncertainties. The full error bars represent the quadratic sum of the statistical and systematic uncertainties. In addition there is an overall scale uncertainty of 8.1% due to the uncertainty in the target polarization.

fraction. The uncertainty due to the angular dependence and asymmetry of the background was taken as the difference between a fit with a background with no angular dependence and asymmetry, and one having the same angular dependence and asymmetry as the data. The resulting uncertainty was found to be negligible.

The influence of the net beam polarization of approximately 0.095 was estimated by including the SDMEs for W_{LU} and W_{LT} in the fit. Even if the latter had large uncertainties, the influence on the ones for W_{UT} was negligible. The data presented in Fig. 5 are effectively integrated over all or two of the variables Q^2 , x_B , and t' within the experimental acceptance. The effect of this kinematic averaging was estimated by comparing the results of a Monte Carlo simulation that included a modelled dependence of the asymmetry on these variables with the model input values at the average kinematics. Also this effect was found to be negligible.

In the extraction of the SDMEs the small longitudinal component of the target polarization with respect to the direction of the virtual photon (the average value of $|S_L/P_T|$ was 0.072) was neglected. This component introduces a term $S_L W_{UL}$, which is described by 14 SDMEs. As the value of S_L is small, these SDMEs cannot be determined from the present data. A systematic uncertainty was estimated by using several sets of random values obeying the positivity bounds given in Ref. [11] for these SDMEs, and evaluating the resultant changes. Changes of on average 55% of the statistical uncertainty were found, with a maximum of 76% for one SDME ($\text{Im}(s_{++}^{-+} + \epsilon s_{0+}^{-+})$). This is the main source of systematic uncertainty.

Lastly there are systematic uncertainties arising from misalignment of the detector, detector smearing effects, and bending of the beam and produced charged particles in the transverse holding field of the target magnet. The uncertainties due to all effects together were investigated with a Monte Carlo simulation of the possible influence of these effects. The resultant uncertainty was found to be negligible.

The resulting SDMEs are shown in Fig. 4. Almost all of them are consistent with zero within 1.5σ , where σ represents the total uncertainty in the value of an SDME. Note that these include s-channel helicity conserving SDMEs. Similar SDMEs in the unpolarized case were found [12] to be non-zero and large (0.4 - 0.5). The SDMEs $\text{Im}(s_{0+}^{0+} - s_{0+}^{-0})$, $\text{Im}s_{-+}^{-+}$, and $\text{Im}n_{0+}^{00}$ deviate more than 2.5σ from zero. The former two involve the interference between natural (N) and unnatural (U) parity exchange amplitudes [11]. For instance, $\text{Im}s_{0+}^{0+}$ contains the product $N_{0+}^{0+}(U_{-+}^{++})^*$ and $\text{Im}s_{-+}^{-+}$ contains the product $N_{-+}^{-+}(U_{-+}^{++})^*$. The detailed analysis of unpolarized data has shown that N_{0+}^{0+} and N_{-+}^{-+} are dominant N amplitudes. The U amplitudes presumably are small, as they are suppressed at large Q^2 . However, U_{-+}^{++} is rel-

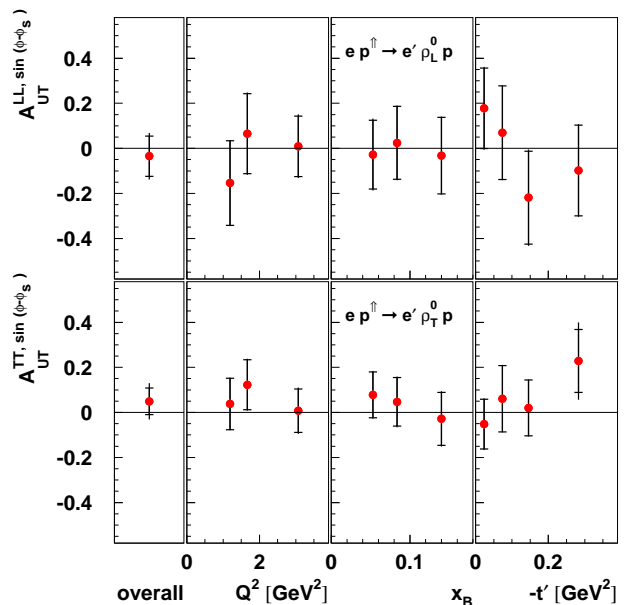


FIG. 5: The extracted amplitudes of the $\sin(\phi - \phi_S)$ component of A_{UT} for longitudinally (top) and transversely polarized (bottom) ρ^0 mesons. The inner error bars represent the statistical uncertainties. The full error bars represent the quadratic sum of the statistical and systematic uncertainties. In addition there is an overall scale uncertainty of 8.1% from the uncertainty in the target polarization.

atively large [12, 20]. The SDME $\text{Im}n_{0+}^{00}$ corresponds to a $\gamma_T^* \rightarrow \rho_L$ transition, the SDMEs of which were found to be non-zero in the unpolarized case. The value of -0.069 ± 0.022 measured for $\text{Im}n_{0+}^{00}$ is another indication of violation of SCHC in the $\gamma_T^* \rightarrow \rho_L$ transition.

As mentioned, the $\sin(\phi - \phi_S)$ term in the transverse target-spin asymmetry for production of longitudinally polarized ρ^0 mesons is of special importance because of its sensitivity to the GPD E . The amplitude of this term is given in terms of SDMEs as [11]

$$A_{UT}^{LL, \sin(\phi - \phi_S)} = \frac{\text{Im}(n_{++}^{00} + \epsilon n_{00}^{00})}{u_{++}^{00} + \epsilon u_{00}^{00}}. \quad (9)$$

The resultant values for all selected data and for bins in x , Q^2 , and t' are shown in Fig. 5 (top). They are all zero within the error bars. Because the SCHC violating terms $\text{Im}(n_{++}^{00})$ and u_{++}^{00} in Eq. 9 require a double helicity flip (see Ref. [11] for details), they presumably can be neglected. Then the value of $A_{UT}^{LL, \sin(\phi - \phi_S)} = -0.035 \pm 0.103$ ² can be compared to the results of GPD calculations for the production of a longitudinally po-

² This is the value for 'all' data, which has average kinematics $\langle Q^2 \rangle = 1.95 \text{ GeV}^2$, $\langle x_B \rangle = 0.08$, and $\langle -t \rangle = 0.13 \text{ GeV}^2$.

larized ρ^0 by a longitudinal photon $A_{UT,\gamma_L^*,\rho_L}^{\sin(\phi-\phi_S)}$, which is given by $\text{Im}(n_{00}^{00})/u_{00}^{00}$.

The $\sin(\phi-\phi_S)$ amplitude for the production of transversely polarized ρ^0 mesons is given by

$$A_{UT}^{TT,\sin(\phi-\phi_S)} = \frac{\text{Im}(n_{++}^{++} + n_{++}^{--} + 2\epsilon n_{00}^{++})}{1 - (u_{++}^{00} + \epsilon u_{00}^{00})}. \quad (10)$$

The values for this asymmetry are shown in Fig. 5 (bottom). Also these are zero within the error bars.

A few groups have performed GPD-based calculations of the transverse target asymmetry for exclusive ρ^0 production. In Refs. [5, 21] the quark GPD E^q is parametrized in terms of the value of J^u , taking $J^d = 0$. Ref. [21] includes the contribution of gluons. The calculated values of $A_{UT,\gamma_L^*,\rho_L}^{\sin(\phi-\phi_S)}$ are in the range 0.15 to 0.00 for $J^u = 0.0$ to 0.4. In Refs. [22, 23] the GPDs are modeled using data for nucleon form factors, sum rules and positivity constraints. The results of both calculations are similar. Values of J^u and J^d of approximately 0.22 and 0.00, respectively, are found, and the calculated values of the asymmetry are very small (-0.03 to 0.02), which is consistent with the present data. It must be realized that the results depend on the modelling of the relevant GPDs of both quarks and gluons, and that the kinematic conditions of the calculations are in several cases outside the kinematic range of the present data.

In summary, the transverse target single-spin asymmetry was measured for exclusive ρ^0 electroproduction on a transversely polarized hydrogen target. Spin density matrix elements were determined by using the angular distributions of the produced ρ^0 mesons and their decay into two pions. Almost all of the SDMEs describing transverse target polarization were found to be consistent with zero. A notable exception is an SDME that corresponds to the production of a longitudinally polarized ρ^0 by a transverse virtual photon. The fact that it is non-zero indicates a small violation of s -channel helicity conservation in the case of a transversely polarized target. The amplitude of the $\sin(\phi-\phi_S)$ component of the asymmetry for the production of longitudinally polarized ρ^0 mesons was found to be small (-0.035 ± 0.103). Neglecting double helicity changing SDMEs, this component can be identified with the leading-twist term of the asymmetry. Calculations based on generalized parton distributions predict small values, consistent with the measured value.

We thank M. Diehl for providing us with the theoretical formalism in an early stage and for many interesting and helpful discussions. We gratefully acknowledge the DESY management for its support and the staff at DESY and the collaborating institutions for their significant effort. This work was supported by the FWO-Flanders, Belgium; the Natural Sciences and Engineering Research Council of Canada; the National Natural Science Foundation of China; the Alexander von Hum-

boldt Stiftung; the German Bundesministerium für Bildung und Forschung (BMBF); the Deutsche Forschungsgemeinschaft (DFG); the Italian Istituto Nazionale di Fisica Nucleare (INFN); the MEXT, JSPS, and COE21 of Japan; the Dutch Foundation for Fundamenteel Onderzoek der Materie (FOM); the U. K. Engineering and Physical Sciences Research Council, the Particle Physics and Astronomy Research Council and the Scottish Universities Physics Alliance; the U. S. Department of Energy (DOE) and the National Science Foundation (NSF); the Russian Academy of Science and the Russian Federal Agency for Science and Innovations; the Ministry of Trade and Economical Development and the Ministry of Education and Science of Armenia; and the European Community-Research Infrastructure Activity under the FP6 "Structuring the European Research Area" program (HadronPhysics, contract number RII3-CT-2004-506078).

-
- [1] D. Müller *et al.*, Fortschr. Phys. 42 (1994) 101.
 - [2] A.V. Radyushkin, Phys. Lett. B 380 (1996) 417, Phys. Rev. D 56 (1997) 5524.
 - [3] X. Ji, Phys. Rev. Lett. 78 (1997) 610, Phys. Rev. D 55 (1997) 7114.
 - [4] J.C. Collins, L. Frankfurt, and M. Strikman, Phys. Rev. D 56 (1997) 2982.
 - [5] K. Goetze, M.V. Polyakov, and M. Vanderhaeghen, Prog. Part. Nucl. Phys. 47 (2001) 401.
 - [6] M. Diehl, Phys. Rep. 388 (2003) 41.
 - [7] A.V. Belitsky and A.V. Radyushkin, Phys. Rep. 418 (2005) 1.
 - [8] M. Diehl and A.V. Vinnikov, Phys. Lett. B 609 (2005) 286.
 - [9] K. Schilling and G. Wolf, Nucl. Phys. B 61 (1973) 381.
 - [10] H. Fraas, Ann. Phys. 87 (1974) 417.
 - [11] M. Diehl, J. High Energy Phys. JHEP09 (2007) 064.
 - [12] A. Airapetian *et al.*, submitted to Eur. Phys. J. C (arXiv:0901.0701v1 [hep-ex]).
 - [13] K. Ackerstaff *et al.*, Nucl. Instrum. Methods A417 (1998) 230.
 - [14] A. Airapetian *et al.*, Nucl. Instrum. Methods A540 (2005) 68.
 - [15] T. Sjöstrand *et al.*, Comput. Phys. Commun. 135 (2001) 238.
 - [16] P. Liebing, Dissertation, Universität Hamburg, September 2004, DESY-THESIS-2004-36.
 - [17] A. Hillenbrand, Dissertation, Friedrich-Alexander-Universität Erlangen-Nürnberg, September 2005, DESY-THESIS-2005-035.
 - [18] B. Maiheu, Ph.D. thesis, Universiteit Gent, March 2006, (HERMES report 06-061).
 - [19] L.N. Hand, Phys. Rev. 129 (1963) 1834.
 - [20] S.I. Manaenkov, HERMES report 06-117 and private communication.
 - [21] F. Ellinghaus, W.-D. Nowak, A.V. Vinnikov, and Z. Ye, Eur. Phys. J. C 46 (2006) 729.
 - [22] S.V. Goloskokov and P. Kroll, arXiv:0708.3569v2 [hep-ph] and Eur. Phys. J. C 59 (2009) 809.
 - [23] M. Diehl and W. Kugler, Eur. Phys. J. C 52 (2007) 933.